JOURNAL OF MOLECULAR SPECTROSCOPY **172**, 303–318 (1995)

The Rotational Structure of the Vibrational States and Substates of Symmetry E in CF_4

SVEND BRODERSEN* AND B. I. ZHILINSKII†

**Department of Chemistry, Aarhus University, Langelandsgade 140, DK-8000 Aarhus C, Denmark; and*
†Laboratoire de Physico-Chimie de l'Atmosphère, Université du Littoral, Dunkerque, France

In continuation of previous papers on the rotational structure of vibrational states in CF_4 (S. G. Larsen and S. Brodersen, *J. Mol. Spectrosc.* **157**, 220–236, 1993 and B. I. Zhilinski, S. Brodersen, and M. Madsen, *J. Mol. Spectrosc.* **160**, 192–216, 1993; and S. Brodersen and B. I. Zhilinskii, *J. Mol. Spectrosc.* **169**, 1–17, 1995) the splitting of the vibrational states or substates of symmetry E is discussed in detail. It is found that all such states split into two vibrational components, the possible symmetries of which were predicted in a previous paper (B. I. Zhilinskii and S. Brodersen, *J. Mol. Spectrosc.* **163**, 326–338 (1994)). In the middle of each double manifold a cluster appears, the position of which determines the symmetries of the two components. The states ν_2, $\nu_1 + \nu_2$, and $3\nu_2(E)$ in all three isotopic species are found to have a central 8_0 cluster which usually belongs to the upper component, causing this to have $D_u^{(J+2)}$ symmetry and the lower to have $D_g^{(J-2)}$ symmetry. For a few J values in the $3\nu_2(E)$ of $^{12}CF_4$ the central cluster belongs to the lower component, causing this to have $D_g^{(J+2)}$ symmetry and the upper component to have $D_u^{(J-2)}$ symmetry. The splitting of the $2\nu_2(E)$ substate is completely different in all three isotopic species. The central 12_0 cluster belongs to the upper component, causing this to have $D_g^{(J+4)}$ symmetry and the lower to have $D_u^{(J-4)}$ symmetry. Further possibilities of types of splittings are discussed. Finally, a review is given of the main results of all five papers.

INTRODUCTION

The rotational structure within the vibrational states or substates of symmetry E in spherical top molecules has not been described experimentally or theoretically in the same detail as has been done for the states of symmetry F_2. Using semiclassical theory Harter *et al.* (*1*) in 1978 calculated the basic cluster pattern for the ν_2 fundamental state of a general spherical top molecule from an approximate effective Hamiltonian operator. However, they used effective Hamiltonians that were too simplified to be able to compute any splitting. By adding one extra term to the effective Hamiltonian, Sadovskii and Zhilinskii (*2*) in 1988 predicted a splitting into two vibrational components.

The present study of four vibrational states or substates of symmetry E in $^{12}CF_4$, $^{13}CF_4$, and $^{14}CF_4$ is a continuation of previous studies of the rotational–vibrational structure of the 10 lowest vibrational states in CF_4 (*3–5*). It is based on a very accurate Hamiltonian, including a potential fitted to almost all experimental data, and the corresponding method of calculation allows a much more accurate study, not only of the ν_2 state, but also of the $\nu_1 + \nu_2$ state and the E substates of $2\nu_2$ and $3\nu_2$ in all three isotopic species of CF_4.

Recently (*5*) it was shown that many interactions between neighboring vibrational components in CF_4 may be interpreted as the result of a transfer of one or more clusters between the components. One of the results of the present work is that all the E states are split into two components by a mechanism which may be interpreted as one-half of such a transfer of one cluster with $J_x \approx 0$.

0022-2852/95 $12.00

In another recent paper (*6*) it has been shown that a vibrational state or substate of symmetry E in principle may split into two components in many different ways, the four most probable solutions being a split into two components of symmetries

$$\begin{array}{llll} \text{(A)} & D_u^{(J+2)} \text{ and } D_g^{(J-2)}, & & \\ \text{(B)} & D_u^{(J-2)} \text{ and } D_g^{(J+2)}, & & \\ \text{(C)} & D_g^{(J-4)} \text{ and } D_u^{(J+4)}, & \text{or} & \\ \text{(D)} & D_g^{(J+4)} \text{ and } D_u^{(J-4)}. & & \end{array}$$

It was also shown that if an E state is split according to solution A, a transfer of one 8-fold cluster from the component with symmetry $D_u^{(J+2)}$ to the component with symmetry $D_g^{(J-2)}$ results precisely in solution B. Likewise, if an E state is split according to solution B, a transfer of one 8-fold cluster from the component with symmetry $D_g^{(J+2)}$ to the component with symmetry $D_u^{(J-2)}$ results precisely in solution A. Likewise, if an E state is split according to solution B, a transfer of one 12-fold cluster from the component with symmetry $D_g^{(J+2)}$ to the component with symmetry $D_u^{(J-2)}$ results precisely in solution D.

In the following discussion it will be demonstrated how these theoretical results may be utilized to interpret the splitting of any of the 12 E states studied here as one-half of such a transfer, either of one 8-fold cluster or of one 12-fold cluster.

THE ν_2 AND $\nu_1 + \nu_2$ STATES

The rotational structure of the ν_2 state of $^{12}CF_4$ was discussed previously (*3, 4*), and it was indicated that it is split according to solution A given above. Here, a more detailed discussion is given of this splitting.

The rotational structure of both components for $J = 22$ is given in Fig. 1. It shows a clear splitting into a low energy component of symmetry $D_g^{(J-2)}$ and a high energy component of symmetry $D_u^{(J+2)}$. The lower component has a type I pattern of clusters (*3*) with a well developed series of 6-fold clusters at the low energy end of the manifold and a very short series of only one 8-fold cluster at the high energy end. The higher component has a type II pattern of clusters, opposite to that of the lower component. This means that both components have a series of 8-fold clusters toward the gap between the two components. Table I indicates the k-distributions of these 8-fold clusters. By comparison with Table I of Ref. (*5*) it is clear that these k-distributions appear to be caused by a rearrangement of cluster indices due to a transfer of the central cluster at 531.943 cm^{-1} from one component to the other. However, there is no such transfer to be observed from the energy level diagram for a large number of J values. There is constantly a larger energy gap below the central cluster than above it, clearly indicating the same separation into vibrational components for all J.

Figure 2 is a plot, as a function of J, of the k-distributions for $J - k = 0$ for the two 8-fold clusters nearest to the central cluster. This plot is thus analogous to each of the two plots shown in Fig. 3 of Ref. (*5*), except that in the present case it is possible to show the values for both neighboring clusters. Figure 2 illustrates that the k-distributions do indeed change as by a real transfer, with a value of $J_{\times 8}$ close to zero, and a redistribution taking place over a very wide range of J values. In the upper component the neighboring cluster disappears for $J \geqslant 40$ because of the complex inversion starting around this J value (*4*), but in the lower component the rearrangement goes on slowly for all J up to 70, where our data stop. Even at this high J the k-distribution has not

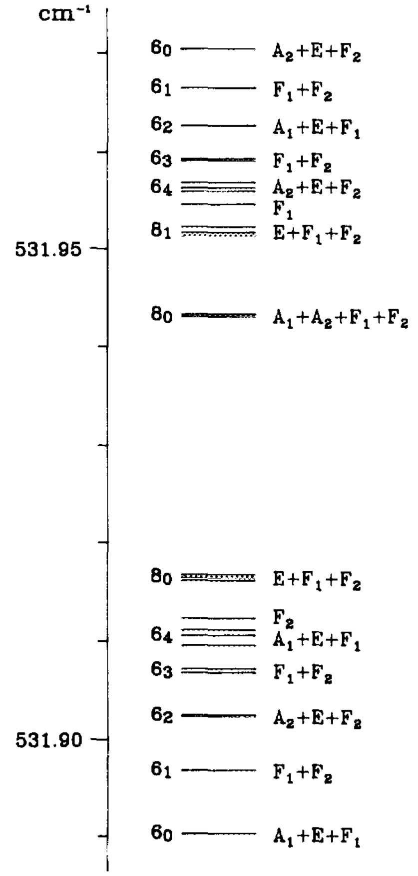

FIG. 1. The energy level diagram of the ν_2 vibrational state of $^{12}CF_4$ for $J = 22$, showing the central 8_0 cluster and the splitting into two vibrational components.

become ideal, as indicated by the values of 0.950 for the k-distribution for $J - k = 0$ and of 0.041 for $J - k = 1$.

If an 8-fold cluster were indeed transferred from the upper component of symmetry $D_u^{(J+2)}$ to the lower component of symmetry $D_g^{(J-2)}$, the result would be an upper component of symmetry $D_u^{(J-2)}$ and a lower component of symmetry $D_g^{(J+2)}$, as stated above. In other words, the position of the central 8-fold cluster determines the choice

TABLE I

The k-Distributions of the 8-fold Clusters in the ν_2 State of $^{12}CF_4$ for $J = 22$

E	Symmetry	τ	k-distribution x 1000					
cm^{-1}			J–k = 0	1	2	3	4	5
531.952	$E+F_1+F_2$	1	314	603	21	43	80	55
531.943	$A_1+A_2+F_1+F_2$	0	984	1	2	15	5	9
531.916	$E+F_1+F_2$	0	646	315	8	21	41	29

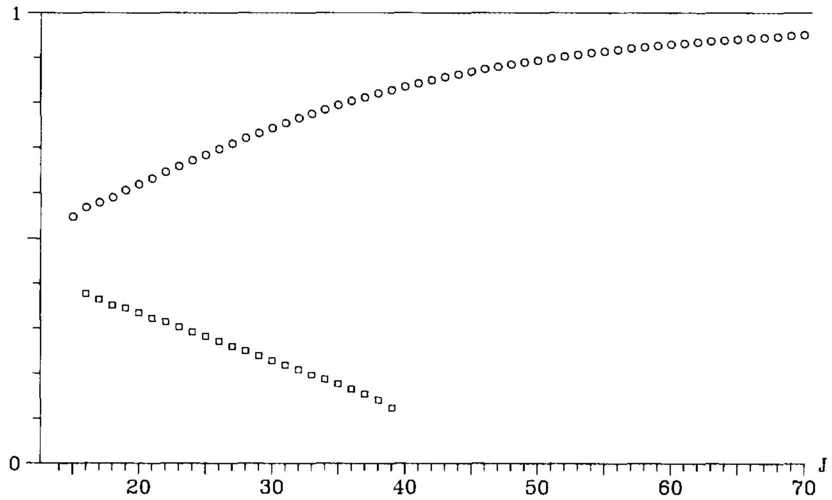

FIG. 2. The k-distributions for $J - k = 0$ for the two 8-fold clusters nearest to the central cluster of the ν_2 vibrational state of $^{12}CF_4$, as a function of J. The cluster belonging to the lower component is symbolized by a circle; that from the upper component by a square.

between the two solutions A and B. This is illustrated in Fig. 3. If the J axis had been of the usual kind from left to right, the diagram would illustrate this ordinary effect of the transfer of the 8-fold cluster. However, the splitting of the two components is due only to one-half of a transfer of the 8-fold cluster, and the J axis in Fig. 3 accordingly starts at $J_{\times 8}$ in the middle of the diagram and proceeds toward solution A. Thus, only the right half of the diagram is relevant in the present case.

Because of the special role of the central 8-fold cluster, it seems reasonable to discuss the structure of the two components as consisting of the lower component, the central cluster, and the remaining parts of the upper component. A special kind of symmetry is then observed, as exemplified in Fig. 1. Not only is the number of 6-fold clusters, etc., the same, but the symmetries are also symmetrical for all states, except for an interchange of the subscripts 1 and 2. The lower component has the symmetry $D_g^{(J-2)}$, and the remaining parts of the upper components have the symmetry $D_u^{(J-2)}$, as indicated in the lower right-hand corner and the upper left-hand corner of the diagram in Fig. 3, respectively. The interchange of subscripts 1 and 2 corresponds

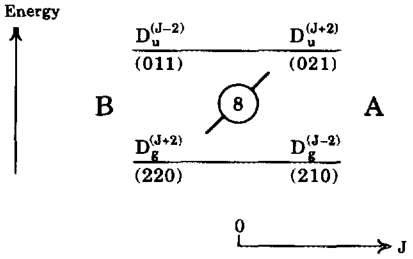

FIG. 3. A diagram showing how the splitting of the ν_2, $\nu_1 + \nu_2$, and $3\nu_2(E)$ states may be interpreted as due to half a transfer of an 8-fold cluster. The right-hand side of the diagram corresponds to solution A, the left hand side to solution B.

to the difference between the subscripts u and g for the symmetries. Even the energy differences in the two reduced components are roughly symmetrical. We refer to this phenomenon as a pseudosymmetry of the vibrational state. It is observed for the ν_2 state from $J = 2$ where the $D_g^{(J-2)}$ component starts up to about $J = 35$ where the energy gap between the two components has increased to a large value. This pseudosymmetry is always exact, even with respect to the energies, if the approximate Hamiltonian of Harter *et al.* (*1*) is used. The splitting and the asymmetry appear only when further terms are added (*2*).

The cluster structure of the ν_2 state of the $^{13}CF_4$ and $^{14}CF_4$ molecules are almost identical to that of the $^{12}CF_4$ molecule, and the corresponding plots are not distinguishable from the one shown in Fig. 2. This is connected with the fact that the isotopic shifts for the vibrational ν_2 state are only 0.045 and 0.085 cm^{-1} for $^{13}CF_4$ and for $^{14}CF_4$, respectively, and these shifts decrease as J increases, passing zero at $J = 39$. This means that the central C nucleus of the molecule hardly moves for this vibration, causing the pattern of rotational–vibrational states to be almost independent of the mass of the central nucleus.

The $\nu_1 + \nu_2$ states of all three molecules are qualitatively identical to the ν_2 states, the main quantitative difference being that the rearrangement of the k-distributions takes place over an even wider range of J values. Thus at $J = 70$ the k-distribution for $J - k = 0$ of the first 8-fold cluster in the lower component in $^{12}CF_4$ has only reached a value of 0.787 compared to 0.950 for ν_2. In the upper component the 8-fold clusters do not disappear, as they do in the ν_2 state due to the complex inversion, which starts at a slightly higher J value in the $\nu_1 + \nu_2$ state. It is possible to follow the central cluster and the neighboring one even to $J = 70$, and the redistribution follows the usual pattern, although the values for the k-distributions are influenced slightly by the inversion.

THE $3\nu_2(E)$ SUBSTATES

The $3\nu_2(E)$ substates of the $^{13}CF_4$ and $^{14}CF_4$ molecules are almost identical to the $\nu_1 + \nu_2$ states, whereas that of the $^{12}CF_4$ molecule is quite different. The k-distributions for $J - k = 0$ for the two 8-fold clusters nearest to the central cluster for $^{12}CF_4$ are shown in Fig. 4. For $J < 30$ the separation into two vibrational components is as usual according to solution A, but the difference between the two k-distributions is very small, and the central cluster is correspondingly placed almost in the center of the pattern of energy levels, with a slight preference for the upper component. This very small difference becomes even smaller for $J > 30$ until at $J = 41$ the difference changes sign, and the central cluster correspondingly is closer to the lower component. This means that for $J \geqslant 41$ the upper component has $D_u^{(J-2)}$ symmetry, and the lower component has $D_g^{(J+2)}$ symmetry, and the substate is thus split according to solution B. In terms of the diagram given in Fig. 3, this corresponds to a change from the right-hand side of the diagram to the left-hand side as J increases through the value of 41. The data given in Fig. 4 stop at $J = 47$ because a complex inversion takes place as usual in the upper component for $J \geqslant 46$, causing the 8-fold clusters to disappear.

At $J \approx 53$ both components are crossed by the $D_u^{(J+1)}$ component of the ν_3 state, as discussed in Ref. (5). As a result of this crossing the components of $3\nu_2(E)$ again have the usual symmetries, $D_u^{(J+2)}$ for the upper component and $D_g^{(J-2)}$ for the lower component, for $J > 53$. The unusual choice of solution for the splitting is thus only present for a relatively short range of J values. The special pattern of the $3\nu_2(E)$ substate for the $^{12}CF_4$ molecule is connected to the crossing of the one component of

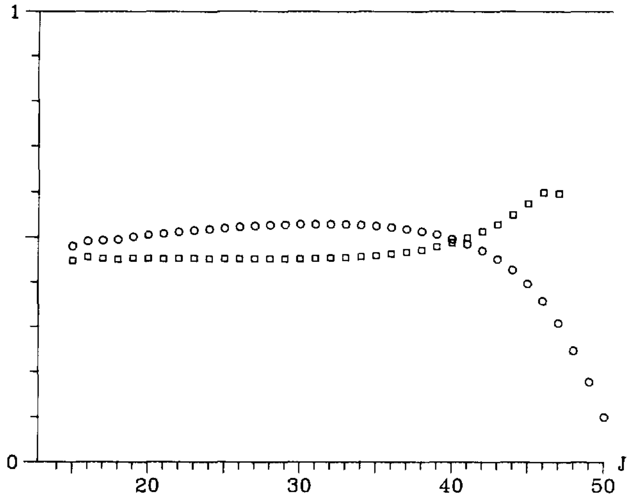

FIG. 4. The k-distributions for $J - k = 0$ for the two 8-fold clusters nearest to the central cluster of the $3\nu_2(E)$ vibrational state of $^{12}CF_4$, as a function of J. The cluster belonging to the lower component is symbolized by a circle, that from the upper component by a square.

the ν_3 state. Such a crossing does not exist for the other two molecules for reasonable values of J.

THE $2\nu_2(E)$ SUBSTATES

The half-a-transfer splitting with a central 8-fold cluster and the pseudosymmetry are the characteristic features for the nine E (sub)states discussed thus far. In contrast to these, the $2\nu_2(E)$ substates of all the three isotopic molecules show a significantly different pattern. It has previously been stated (*3*) that the $2\nu_2(E)$ substate does not split into vibrational components. This statement is fortunately incorrect. It was, however, correctly indicated that a splitting is observed if the energy level diagram is computed on the basis of the previously published cubic potential (*7*), and such a calculation is the key to an understanding of the unusual pattern in the present case.

It is found that the substate calculated from the cubic potential is split into an upper component of symmetry $D_g^{(J+4)}$, and a lower component of symmetry $D_u^{(J-4)}$, corresponding to solution D indicated above. The pattern of clusters is correspondingly significantly different from that of the ν_2 state. As an example, Fig. 5a gives the energy level diagram for $J = 36$ as calculated from the cubic potential. Two series of 6-fold and 8-fold clusters appear in both components, starting at or near the high energy end of the manifold in the upper component, and at or near the low energy end of the manifold in the lower component. Toward the gap each component has a series of 12-fold clusters. As seen from the k-distributions indicated in Table II, these 12-fold clusters play the same role here as the 8-fold clusters in the previous examples, with the 12_0 cluster at 1124.610 cm^{-1} as the central cluster. Figure 6 is a diagram showing how this splitting may be interpreted as due to half a transfer of a 12-fold cluster, in agreement with the statements given in the Introduction. This diagram also shows that if the central cluster is removed, the remaining components have symmetries $D_u^{(J-2)}$ and $D_u^{(J-4)}$, preventing the appearance of a pseudosymmetry in this case. This

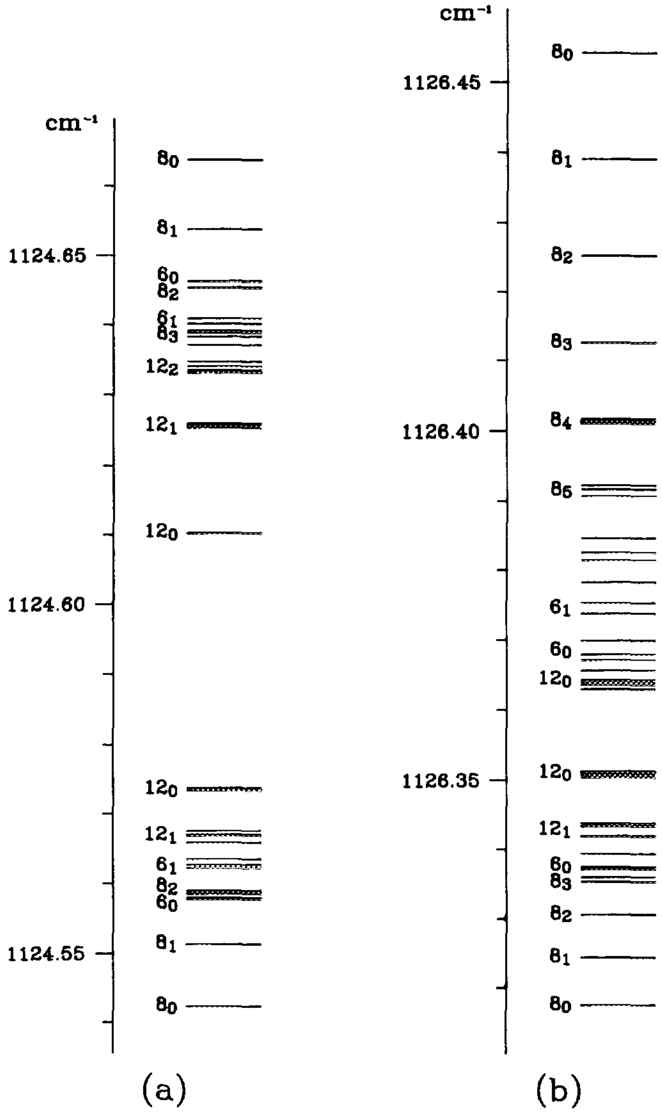

FIG. 5. The energy level diagram of the $2\nu_2(E)$ vibrational state of $^{12}CF_4$ for $J = 36$. (a) is computed on the basis of a cubic potential function (*7*); (b) is computed from the almost true quartic potential.

also means that the central 12_0 cluster cannot appear precisely in the middle of the double manifold.

The corresponding energy level diagram shown in Fig. 5b was computed from the almost true quartic potential (*8*). The lower component is nearly unchanged by this change of potential; only the 6_0 cluster has moved up a bit within the component. The upper component, on the other hand, has changed significantly. The series of 12-fold clusters has shortened to one 12_0 cluster only, the series of 6-fold clusters has turned, and the series of 8-fold clusters has increased in length and is now the dominating feature of the upper component. The most important change is, however, that

TABLE II

The *k*-Distributions of the 12-fold Clusters in the $2\nu_2(E)$ State of $^{12}CF_4$ for $J = 36$ as Computed from a Cubic Potential

E cm^{-1}	Symmetry	τ	k-distribution x 1000 J–k = 0	1	2	3	4	5
1124.634	$A_1+E+F_1+2F_2$	2	60	323	212	196	188	60
1124.626	$A_2+E+2F_1+F_2$	1	356	436	83	113	9	14
1124.610	$A_1+E+F_1+2F_2$	0	902	13	80	1	4	1
1124.574	$A_2+E+2F_1+F_2$	0	538	323	28	103	3	13
1124.567	$A_1+E+F_1+2F_2$	1	13	359	287	86	237	42

the gap between the two components has decreased so much that it has the same order of magnitude as the spacing within the series of 8-fold clusters.

A further change is that the width of many clusters has increased considerably. Thus the width of the central 12_0 cluster has increased by a factor of 27. This is caused by the two components being so close when computed from the quartic potential that they can no longer be treated as isolated components. A similar effect on the *k*-distributions is seen in Table III. A comparison with the corresponding numbers for the cubic potential in Table II shows that the *k*-distribution for the central 12_0 cluster is now very far from ideal, and the effect on the 12_0 cluster of the lower component is so large that the *k*-distribution looks as if it belongs to a 12_1 cluster. The correct assignment of τ is only possible by an extrapolation from the following 12_1 cluster and by use of the symmetry compared to Table IV of Ref. (*3*).

In terms of the semiclassical theory, the C_2 points on the two classical rotational energy surfaces of the two components are extremely close. The gap between the two 12_0 clusters is only 0.012 cm^{-1}. To compute the separation between the C_2 points, we should subtract one-half of the spacing within both of the two series of clusters in order to extrapolate one-half quantum beyond 12_0 in both series, but only 12_0 and 12_1 of one series are seen, and we get the best estimate by subtracting the energy difference of 0.007 cm^{-1} between these two clusters. This results in an estimate of 0.005 cm^{-1} for the separation between the C_2 points. This is even less than the difference of 0.007 cm^{-1} between 12_0 and 12_1, indicating that a strong perturbation is to be expected, at least between the first members of the two series of clusters.

In comparison to this case, the separation of 0.15 cm^{-1} between the C_3 points, again obtained by extrapolation, is many times the spacing in any of the two series of 8-fold

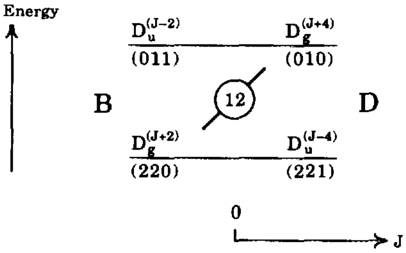

FIG. 6. A diagram showing how the splitting of the $2\nu_2(E)$ state may be interpreted as due to half a transfer of a 12-fold cluster. The right-hand side of the diagram corresponds to solution D, the left hand side to solution B.

TABLE III

The k-Distributions of the 12-fold Clusters in the $2\nu_2(E)$ State of $^{12}CF_4$ for $J = 36$ as Computed from a Quartic Potential

E	Symmetry	τ	k-distribution x 1000					
cm^{-1}			J–k = 0	1	2	3	4	5
1126.364	$A_1+E+F_1+2F_2$	0	420	76	98	71	52	68
1126.351	$A_2+E+2F_1+F_2$	0	249	411	1	204	7	88
1126.343	$A_1+E+F_1+2F_2$	1	62	262	202	52	256	30

clusters, and these appear practically unperturbed with respect to the widths, to the spacing, and to the k-distributions. This is an interesting observation, allowing the general conclusion that even though two classical energy surfaces are extremely close at certain points, the series of clusters connected with other points at the surfaces may in every respect behave as if the two components were completely isolated. In fact, this case is rather similar to the case of a simple overlap of the two surfaces, where the clusters of the two components overlap, although the two surfaces are well separated for any direction of the angular momentum. This case also leads to no perturbation between the clusters of the two components.

The C_4 points represent an intermediate case. The separation between the C_4 points is about 0.03 cm^{-1} which is five times the spacing between the two 6-fold clusters of the upper component. Correspondingly, the clusters have broadened a little and the k-distributions are less ideal, but these effects are not nearly as prominent as those for the 12-fold clusters.

For $J < 36$ the pattern of clusters is in principle the same as the one shown in Fig. 5b, although, of course, the number of clusters must decrease as J decreases. Thus, all three series of clusters are only present in both components for $J \geqslant 25$ which makes it difficult to understand the basic structure if the energy level diagram is found only for some J value below 25.

What happens for $J > 36$ is shown in Fig. 7, indicating the central part of the energy level diagrams for $37 \leqslant J \leqslant 49$, leaving out primarily the major part of the regular series of 8-fold clusters in the upper component. The most important difference between these diagrams and that for $J = 36$, shown in Fig. 5b, is that the central 12-fold cluster for $J > 36$ is no longer the cluster of lowest energy in the upper component. Between $J = 36$ and $J = 37$ it changes place with the 6_0 cluster, between $J = 41$ and $J = 42$ it changes place with the 6_1 cluster, and at about $J = 44$ it disappears, leaving the upper component to have a simple type I pattern of clusters for $J \geqslant 45$, with a long series of 8-fold clusters starting from the high energy end of the manifold and a much shorter series of 6-fold clusters starting from the low energy end of the manifold.

The gap between the two components is still very small. It reaches a maximum of only 0.0124 cm^{-1} at $J = 39$, then decreases with increasing J, until at $J = 49$ the two components overlap, with the 12_0 cluster of the lower component having higher energy than the 6_0 cluster of the upper component. This does not mean, however, that the two classical energy surfaces touch or cut each other. The energy of the C_2 points of the upper surface is, in the absence of a series of 12-fold clusters, somewhere in the region between the series of 8-fold clusters and that of 6-fold clusters, probably close to 872.30 cm^{-1} in Fig. 7. The energy of the C_2 points of the lower component is found by extrapolation of the series of 12-fold clusters by one-half quantum, leading to an

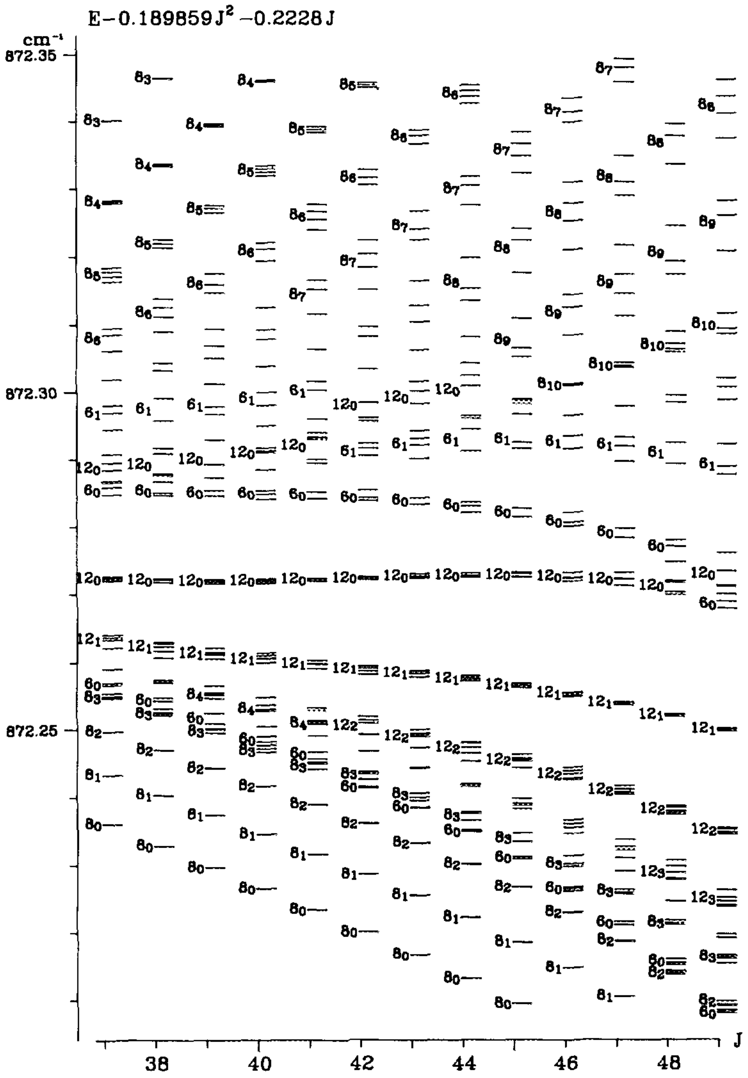

FIG. 7. The central part of the energy level diagram of the $2\nu_2(E)$ vibrational state of $^{12}CF_4$ for $J = 37$–49, computed from the almost true quartic potential function.

energy of about 872.29 cm^{-1} in Fig. 7. The distance at the C_2 points is thus only on the order of 0.01 cm^{-1}, but probably larger than for $J = 36$. Extrapolating the two series of 8-fold clusters, the distance at the C_3 points is determined to be 0.37 cm^{-1}, and the distance at the C_4 points is correspondingly found to be about 0.06 cm^{-1}. This means that the two surfaces do not touch each other. But the C_4 points of the upper surface represent a lower energy than the C_2 points of the lower surface, and this leads to the overlap of the two components. This is, however, a simple overlap which does not lead to any perturbation of the cluster pattern.

This overlap increases with increasing J, as shown in Fig. 8. There is, however, no problem in assigning all levels to the right component, if one only remembers that all

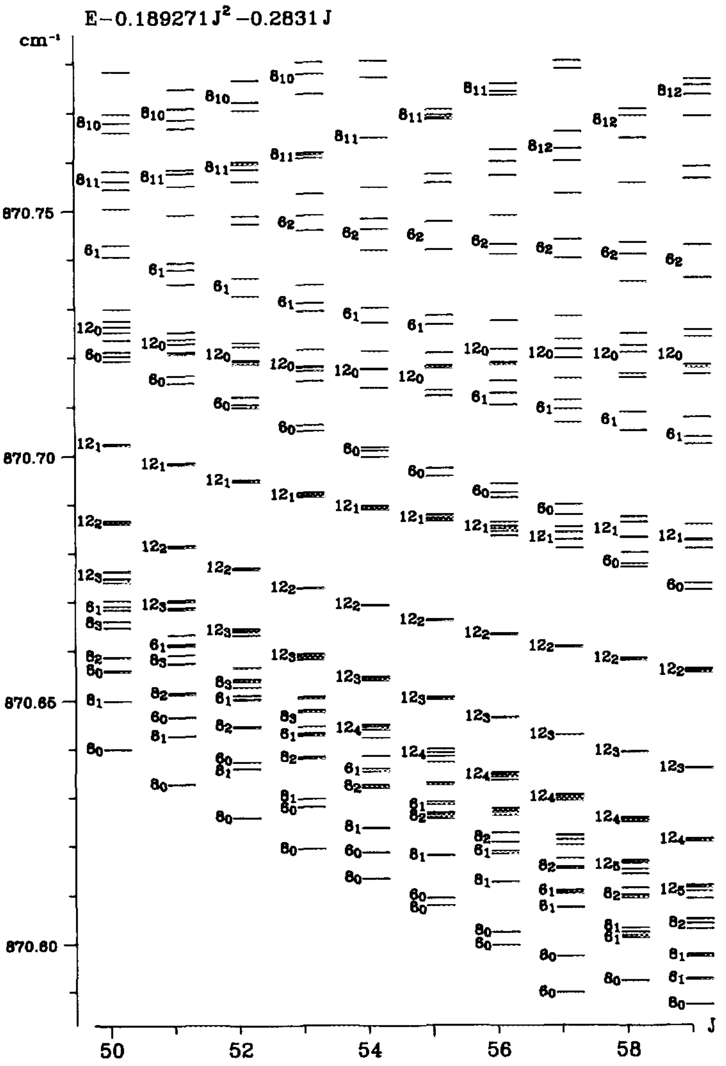

FIG. 8. The central part of the energy level diagram of the $2\nu_2(E)$ vibrational state of $^{12}CF_4$ for J = 50–59, computed from the almost true quartic potential function.

12-fold clusters belong to the lower component, and that this series overlaps the series of 6-fold clusters belonging to the upper component.

The series of 12-fold clusters develops as J increases, including at $J = 59$ six members, which is an unusually high number for a series of 12-fold clusters. The k-distributions are given in Table IV, indicating that the first two clusters are just as heavily perturbed as for J = 36, as seen by comparison with Table III. The explanation is, of course, that the C_2 points still are very close compared to the spacing of the series. Because no 12-fold clusters are seen in the upper component, the energy of the C_2 points of the upper surface is somewhere within the region of no clusters between the 6_2 and 8_{12} clusters. The energy of the C_2 points of the lower surface is also difficult to indicate precisely because the series is so non-equidistant. Probably, it is slightly above the 6_2

TABLE IV

The *k*-Distributions of the 12-fold Clusters in the $2\nu_2(E)$ State of $^{12}CF_4$ for $J = 59$

E	Symmetry	τ	k-distribution x 1000						
cm^{-1}			J–k = 0	1	2	3	4	5	6
1546.276	$A_1+E+F_1+2F_2$	0	201	389	27	108	29	50	29
1546.239	$A_2+E+2F_1+F_2$	1	37	291	349	4	127	19	44
1546.211	$A_1+E+F_1+2F_2$	2	8	78	338	315	1	146	13
1546.191	$A_2+E+2F_1+F_2$	3	1	20	113	349	267	8	163
1546.177	$A_1+E+F_1+2F_2$	4	0	2	31	135	340	226	20
1546.166	$A_2+E+2F_1+F_2$	5	0	0	4	40	146	319	195

cluster. Consequently, the distance between the C_2 points is smaller than the spacing of the series of clusters, and the clusters with low values of τ must be heavily perturbed.

For $J \geqslant 60$ to $J = 70$, where our data stop, the pattern shown in Fig. 8 just develops further. The overlap of the two components increases until at $J = 70$ it is 0.17 cm^{-1}. As may be seen from Figs. 5b, 7, and 8, the series of 6-fold clusters in the lower component is represented for $36 \leqslant J \leqslant 41$ only by the 6_0 cluster placed close to the region of no clusters. For $42 \leqslant J \leqslant 49$ it moves downward relative to the series of 8-fold clusters. For $J \geqslant 50$ a 6_1 cluster appears, and for $J \geqslant 56$ the 6_0 cluster is the cluster of lowest energy within the lower component. This development continues for $60 \leqslant J \leqslant 70$, until at $J = 70$ the series of 6-fold clusters dominates the lower half of the lower component with six members, whereas the series of 8-fold clusters, which dominates for lower J values, is represented by an 8_0 cluster only, placed at the edge of the region of no clusters. This means that for $J = 70$ the last sign of symmetry between the two components, a dominating series of 8-fold clusters at the wings, has disappeared completely. It is also worth to mention that there is no sign of an inversion of the upper component, as seen in ν_2, $\nu_1 + \nu_2$, and $3\nu_2$. It should be noted, however, that this complex inversion just leads to a type I pattern, observed here in the upper component for all values of J larger than 45.

The structure of the $2\nu_2(E)$ substate is very nearly the same for $^{13}CF_4$ and for $^{14}CF_4$. As for ν_2 the isotopic shifts for the vibrational state $2\nu_2(E)$ are small, only 0.102 and 0.191 cm^{-1} for $^{13}CF_4$ and for $^{14}CF_4$, respectively, and these shifts decrease as J increases, passing through zero at $J = 60$. This indicates that the central C nucleus of the molecule also hardly moves for the $2\nu_2(E)$ vibration, causing the pattern of the rotational–vibrational states to be practically independent of the mass of the central nucleus.

TYPES OF SPLITTINGS OF *E* STATES

In the previous sections two significantly different types of splittings of E states have been discussed in detail. It seems an interesting question as to whether even more types of splittings are possible. The key to an answer to this question is the kind of diagram shown in Figs. 3 and 6.

Each of these diagrams represents two types of splittings, according to the direction of the J arrow. As shown in Fig. 3 the J arrow indicates the usual type of splitting corresponding to solution A and a central 8-fold cluster. If, however, the J arrow is reversed, pointing from the middle of the diagram to the left, it indicates the slightly different type of splitting observed in the $3\nu_2(E)$ substate of $^{12}CF_4$ for $41 \leqslant J \leqslant 47$, leading to solution B and a central 8-fold cluster. Likewise, the diagram shown in Fig.

6 indicates the completely different type of splitting observed in the $2\nu_2(E)$ substate, leading to solution D and a central 12-fold cluster. If the J arrow is reversed in this diagram, a new type of splitting is indicated with a central 12-fold cluster and the solution B for the symmetries of the two components. This type of splitting has not been observed within the present data. Strictly speaking, however, each diagram represents four types of splittings, if the energy arrow is also reversed, permuting the symmetries of the lower and the upper components.

If for the moment we concentrate on the four solutions A, B, C, and D, it is possible to construct a total of five diagrams, as shown in Fig. 9, where both the J arrow and the energy arrow have been left out. Of these diagrams, (a) and (b) are those already shown in Figs. 3 and 6, respectively. Each of the remaining three diagrams represents four new types of splittings of an E state. They are all based on the same fundamental concept of half a transfer of one cluster (or, in the last two diagrams, two clusters) between two vibrational components, forming one of the four solutions A, B, C, or D. The two diagrams (b) and (c) show that all four solutions may result with a central 12-fold cluster. Similarly the two diagrams (d) and (e) show that all four solutions

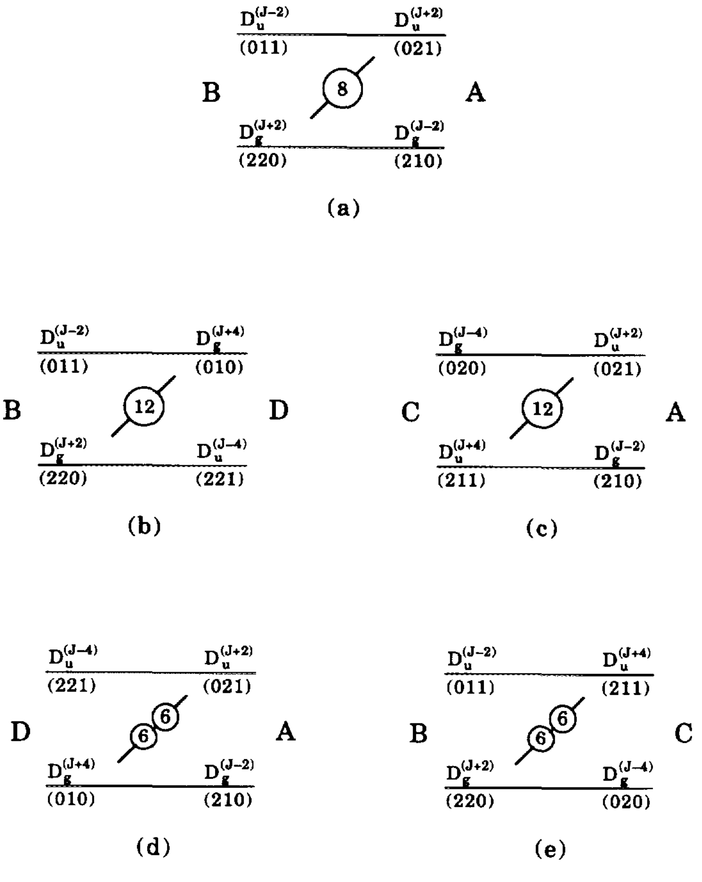

FIG. 9. Five diagrams indicating 20 different types of splittings of E states into vibrational components having the symmetries given by the four solutions A, B, C, and D defined in the text. Each diagram is analogous to the diagrams shown in Figs. 2 and 6, leaving out the axes in order to indicate 4 types of splittings by each diagram.

may result with two central 6-fold clusters. But with a central 8-fold cluster only the two simplest solutions A and B may result, as shown by diagram (a). This diagram is also the only one allowing a pseudosymmetry to appear, because it is the only one indicating symmetries in the upper left-hand corner and the lower right-hand corner differing only in the index g or u. Thus, from a theoretical point of view the diagram (a) represents an exception, but experimentally it is the most common, undoubtedly because of the low value of 2 for the absolute value of Δ in the solutions A and B.

If the two solutions with $|\Delta| = 8$ are included as E and F, it is possible to construct two new diagrams, both with a central 8-fold cluster, the one with a choice between the solutions C and E, and the other with a choice between the solutions D and F. These two diagrams are both analogous to the diagram (a), and for both there is no possibility of a pseudosymmetry.

If the two solutions with $|\Delta| = 10$ are included next as G and H, it is possible to construct four new diagrams, analogous to the diagrams (b), (c), (d), and (e), with a choice in each case between on the one hand the solutions C and D, and on the other the solutions G and H.

Theoretically, one may continue infinitely in this way, indicating that in principle, any E state may split in an infinite number of ways. But the higher the value of $|\Delta|$ becomes, the less probable are the solutions and the corresponding new types of splittings.

CONCLUSION

In this section an attempt is made to review the main results, not only from the present paper, but also from the previous papers (*3–6*) on the rotational structures of the vibrational states of CF_4.

Any degenerate vibrational state may split in two ways. If the vibrational symmetry is given by a sum of symmetries, it splits by anharmonicity in vibrational *substates*, the symmetry of each substate being given by one term in this sum. If the symmetry of a vibrational state or a substate is degenerate, it splits into as many *vibrational components* as given by the degeneracy. The collection of rotational–vibrational states for one value of J within one vibrational component is called a *manifold*.

A vibrational component is primarily characterized by a symmetry $D_g^{(J+\Delta)}$ or $D_u^{(J+\Delta)}$ in the full rotational group O_3, where Δ is a constant number equal, in the observed cases, to 0, ±1, ±2, ±3, or ±4. The well-known correlation from O_3 to T_d indicates immediately the symmetries in T_d of all the rotational-vibrational states within any manifold of the vibrational component. The symmetry of a vibrational component may alternatively be characterized by the *local symmetry indices* (n_4, n_3, n_2). Two methods, one for each way of indicating the symmetry, are given for finding which symmetries are possible for the vibrational components into which a vibrational state or substate of a given symmetry is split.

The dominating feature of the rotational structures is the formation of *clusters* of rotational–vibrational states. Each cluster may be characterized by its degeneracy, its symmetry, and its *cluster index* τ. The degeneracy of a cluster is the sum of the degeneracies of each state. It may be 6, 8, 12, or 24. The symmetry of the cluster is correspondingly the sum of the symmetries of each state. The symmetry of a 24-fold cluster is always $A_1 + A_2 + 2E + 3F_1 + 3F_2$. For the clusters of lower degeneracy, this sum is split into different possible symmetries. The cluster index τ is defined on the basis of the sum of the k-distribution for each state. The k-distribution indicates the weighting of the rotational wavefunctions with different k values, as computed from the eigenvector matrix of the Hamiltonian matrix. This sum of *k*-distributions shows some characteristic peaks, from which the cluster index is unambiguously defined in ideal cases. The determination of the cluster index for less ideal cases is discussed in a number of examples. A connection between the degeneracy, the symmetry, the cluster index τ, J, and the symmetry of the vibrational component is given in Table IV in Ref. (*3*).

The discussion of the pattern of clusters within each manifold is based on the well-known semiclassical theory, the definitions of which are sharpened a little. For each manifold a classical *rotational energy surface* is defined, indicating the classical rotational energy as a function of the direction of the angular momentum given in a molecule-fixed coordinate system. This surface has O_h symmetry, and may be divided into 48 identical spherical triangles, the vertices of which are the 6 equivalent C_4 points, the 8 equivalent C_3 points, and the 12 equivalent C_2 points in which the surface is cut by the 3 C_4 axes, the 4 C_3 axes, and the 6 C_2 axes, respectively. Any point inside the triangle is one of 48 equivalent C_1 points. If the surface has a sufficiently prominent maximum or minimum in such a set of equivalent points, a series of clusters are formed, all having the degeneracy of the points, and with cluster indices $\tau = 0, 1, 2, \ldots$. A discussion of the possible shapes of the rotational energy surface leads to the conclusion that any manifold must contain one such series of 6-fold clusters and one series of 8-fold clusters, out of which one may be so short that it is not observed. Further, one series of 12-fold clusters may appear, and in special cases also a series of 24-fold clusters.

The two most common patterns of clusters within one manifold are termed *type I* and *type II*. In both cases the manifold contains one series of 6-fold clusters and one series of 8-fold clusters. In type I the series of 6-fold clusters starts at the low energy end of the manifold, and the series of 8-fold clusters starts at the high energy end of the manifold. The two series proceed toward the middle of the manifold, the clusters becoming broader and finally disappearing in the region where the two series meet. In type II manifolds the order of the two series is reversed. The classical rotational energy surface has in the case of a type I pattern minima at the 6 C_4 points, responsible for the series of 6-fold clusters, and maxima at the 8 C_3 points, responsible for the 8-fold clusters. For type II it has maxima at the C_4 points and minima at the C_3 points.

The pattern of clusters in the manifolds of one vibrational component as a function of J is discussed in some detail. In a number of cases all manifolds are of type I or in a few cases of type II. In most cases, however, the pattern changes as a function of J. For isolated components these changes may always be explained as a complete or a partial inversion of the pattern from type I to type II, or vice versa. Two different schemes are found to exist for such inversions, the *simple inversion* and the *complex inversion*.

A detailed explanation of each kind of inversion is given on the basis of how the qualitative shape of the classical rotational energy surface changes as a function of J in each of the two cases. The discussion is based on a detailed topological study of which qualitative shapes are possible, the key point being that the surface is never precisely spherical. The complex inversion is of special interest, first, because it causes some series of clusters to bend, the energy of the clusters having either a maximum or a minimum as a function of the cluster index τ, and second, because 24-fold clusters are formed by collecting as a function of J either four 6-fold clusters or three 8-fold clusters from such a bent series of clusters.

The symmetry of a vibrational component usually does not change as a function of J. It does happen, however, that two components that are close in energy both change symmetry due to a transfer of one cluster from one component to the other. The rules for such transfers are given in detail, formulated either using the conventional symmetry symbols or, more conveniently, the alternative local symmetry indices. It is found that the transferred cluster must have the cluster index $\tau = 0$, and that either a 6-fold, an 8-fold, or a 12-fold cluster may be transferred, provided the symmetries of the two components satisfy certain conditions, making sure that the transferred cluster has $\tau = 0$ in both components. Such a transfer requires a rearrangement as a function of J of the k-distributions in the involved series of clusters, reestablishing the usual order of the cluster index in both series.

Examples of such transfers are given, including a detailed discussion of the rearrangement of the k-distributions and of τ. These examples include the important case of components crossing in energy as a function of J. It is shown that the components do not actually cross; instead they exchange symmetry due to the transfer. Likewise the classical rotational energy surfaces do not cross, but only touch each other, which is what causes the transfer of the cluster to take place. In theory two 6-fold clusters might also be transferred, but no example of this has yet been observed.

In the present paper, it is shown how the splitting of any vibrational state or substate of symmetry E may also be interpreted as due to a transfer of one cluster, but only one-half, the transfer itself taking place for $J \approx 0$. The corresponding rearrangement of the k-distributions takes place over a very wide range of J values. An infinite number of different types of splitting are possible, but only a few of these have been observed.

RECEIVED: February 1, 1995

REFERENCES

1. W. G. HARTER, H. W. GALBRAITH, AND C. W. PATTERSON, *J. Chem. Phys.* **69**, 4888–4895 (1978).
2. D. A. SADOVSKII AND B. I. ZHILINSKII, *Mol. Phys.* **65**, 109–128 (1988).
3. S. G. LARSEN AND S. BRODERSEN, *J. Mol. Spectrosc.* **157**, 220–236 (1993).
4. B. I. ZHILINSKII, S. BRODERSEN, AND M. MADSEN, *J. Mol. Spectrosc.* **160**, 192–216 (1993).
5. S. BRODERSEN AND B. I. ZHILINSKII, *J. Mol. Spectrosc.* **169**, 1–17 (1995).
6. B. I. ZHILINSKII AND S. BRODERSEN, *J. Mol. Spectrosc.* **163**, 326–338 (1994).
7. S. BRODERSEN, *J. Mol. Spectrosc.* **145**, 331–351 (1991).
8. S. BRODERSEN, to be published.